01 Dec 2012

Explosively Formed Projectile Soft-Recovery Force Analysis

Laurin Bookout

Phillip R. Mulligan
Missouri University of Science and Technology, pmulligan@mst.edu

Jason Baird
Missouri University of Science and Technology, jbaird@mst.edu

The 12th Hypervelocity Impact Symposium

Explosively Formed Projectile Soft-Recovery Force Analysis

Laurin Bookout[a1], Phillip Mulligan[b], Jason Baird[b]

aApplied Research Associates, 2760 Eisenhower Ave., Suite 308, Alexandria, VA 22304, USA
bMissouri University of Science & Technology, 226 McNutt Hall, Rolla, MO 65409, USA

Abstract

The design of a soft-recovery system is critical to a researcher's ability to analyze hypervelocity projectiles. The researcher may decide to use one method over another based on several criteria, including whether or not non-deformed projectile measurements are required. This report analyzes the forces two different soft-recovery methods impart on the projectiles collected. Method 1 utilized three polyethylene water barrels placed "end-to-end" horizontally, providing 2.6 meters (9 feet) of water to stop the projectile. Method 2 is a modification of the soft-recovery method utilized in "Soft-Recovery of Explosively Formed Penetrators" by Lambert and Pope [1]. This method utilizes a series of several materials with an increasing density gradient, placed end-to-end over 14.3 meters (47 feet) to stop the projectile. Despite the fact that explosively formed projectiles (EFPs) of the same design were fired into each recovery method, the projectiles collected using the two methods differed in shape, size, weight, and the number of pieces collected. Since the EFP designs were identical to begin with, the physical differences are most likely due to the different magnitudes of the forces exerted on the projectile during deceleration. Drag force calculations will be performed for both recovery methods in an attempt to determine the differences in the drag forces exerted on the projectile during its deceleration. The results of the calculations will assist in determining to what extent the physical deformation of the projectile is due to the material selection of each recovery method. The consistency of the shapes and weights of the recovered projectiles will also be briefly addressed to assist the researcher in choosing the most useful recovery method for a given objective.
© 2013 The Authors. Published by Elsevier Ltd. Open access under CC BY-NC-ND license.
Selection and peer-review under responsibility of the Hypervelocity Impact Society
Keywords: Explosively formed projectile, soft recovery, deformation, force, EFP

Nomenclature

A	area (m^2)
C$_D$	Total Drag coefficient
D	Diameter of Projectile (m)
E$_f$	Elastoplastic deformation energy associated with the impact of two masses (kg*m^2/sec^2)
KE	Kinetic Energy (kg*m^2/sec^2)
L	Length of segment (m)
m	Mass of target driven from the plate due to the impact of the projectile (kg)
M	Initial mass of the projectile (kg)
T	Target thickness (m)
V	Projectile velocity (m/sec)
W	Work imparted on the projectile (kg*m^2/sec^2)
Greek symbols	
β	Impact angle between the projectile and target (degrees)
ρ	density
σ$_e$	Linear elastic compressive limit (kg/m*sec^2)
Γ	1.5
Subscripts	
0	Initial

[1]* Corresponding author. Tel.: +1-703-329-0200; fax: +1-703-329-0204.
E-mail address: lbookout@ara.com.

b	Ballistic limit
f	cross-sectional area of the projectile's tail
p	polyethylene

1. Introduction and background

The selection of the appropriate soft recovery method for a projectile depends on the desired data and the limitation of the test facility. Ideally, a soft recovery method slows the projectile gradually by passing it through media of increasing densities, thereby minimizing the force imparted on the projectile by the media. This method results in the collection of a projectile with minimum deformation and reduction of mass due to rapid deceleration [2]. However, one may not always be able to utilize this soft recovery method. This research looks at the projectiles collected from EFPs when fired into two different soft recovery methods.

The soft recovery methods discussed in this paper were designed independently for separate research projects. Each project had different motivating factors during the design process, but required the same EFP design. Method 1's objective was to design a simple soft recovery method that was quick to construct and could provide an approximation of the pre-impact projectile's weight and shape. The objective on method 2 was to obtain an accurate projectile shape and mass for predicting penetration. Upon completion of the projects, the variation of the projectiles' shapes from the two methods called for closer examination of the forces acting on the projectiles due to the recovery methods.

This paper examines the work acting on the projectile to decelerate it, as it traverses the soft recovery methods. The initial velocity and flyer plate mass are used in conjunction with the distance the projectile penetrated into the recovery method to determine the drag coefficients and the magnitude of the force acting on the projectile. A comparison of the forces acting on the projectile will assist in determining how and where in the recovery method the projectiles were deformed. In addition, this paper will address the pros and cons of the two recovery methods in an attempt to assist future researchers in the selection of a recovery method that will suit their needs.

2. Experimental setup

2.1 Explosively Formed Projectile Construction

The EFP design utilized in this research was obtained from previous research at Missouri University of Science and Technology (Missouri S&T), formerly University of Missouri-Rolla [3]. This EFP design consists of a 10 cm (4 in) Polyvinyl chloride (PVC) cylindrical, with PVC end caps. The flyer plate consists of a 0.64 (0.25 in) cm thick copper plate with a radius of curvature of 9.525 cm (3.75 in) see Fig. 1.a. The EFPs were hand packed with a predetermined amount of C-4 and detonated by inserting a blasting cap 1.27 cm (0.5 in) into the charge.

(a)   (b)

Fig. 1. Illustration of the EFP design (a) rubber coated flyer plate and (b) the hand packed EFP.

The previous research at Missouri S&T [3-4] shows agreement with Voort and Rhijnsburger conclusions that hand filled EFPs, not made industrially, showed a straight trajectory and very good reproducibility [2]. The EFP design has a velocity of 1252.2 m/sec. Firing the EFP design, previously discussed, into each soft recovery method enabled the analysis of the following recovery methods.

2.2 Method 1

The first method used to recover the projectiles consist of three polyethylene water barrels placed end-to-end horizontally, providing 2.6 meters (9 feet) of polyethylene and water to stop the projectile. Figure 2.a depicts the projectile's path as it travels though the barrels. The Polyethylene has a density of 954 kg/m^3 and the water has a density of 998 kg/m^3.

The stand design consisted of wooden timbers stacked in a crisscross pattern, see Fig. 2.b. The wooden timber design enabled easier leveling of the barrels prior to each test, as well as minimizing the damage to the stand when the first barrel ruptured during each test.

Prior to each shot the barrels were lined up, leveled, and realigned after each subsequent shot as necessary. Barrels were discarded if they were destroyed or punctured during a test. Due to the inability to suspend the projectiles in the water, the penetration depths could only be estimated at 0.9m increments unless the projectile is stopped in one of the polyethylene layers. All EFPs were placed at a standoff of 3.7 m (12 ft) and the speeds were recorded using a Phantom V5.1 high-speed camera and reference board. Figure 2 shows a conceptual sketch of the setup and a picture of the setup prior to the first shot.
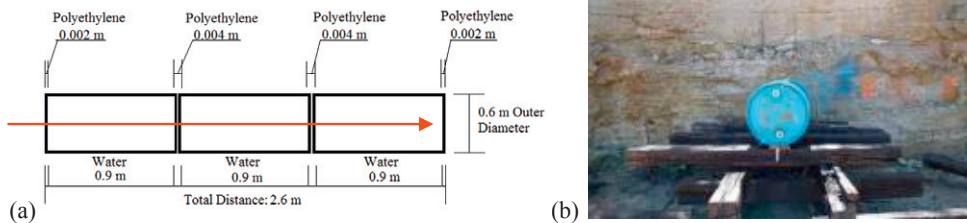

Fig. 2. Illustrates soft recovery method 1 (a) is a side profile of the recovery method with an arrow depicting the projectiles path and (b) is a picture looking at the front of the recovery method.

2.3 Method 2

The second method used to recover the projectiles consisted of a variation on the method developed by Lambert and Pope of the Air Force Research Lab [1]. This method employed a series of materials with increasing densities to slow the projectile down at a more gradual rate than would a single material. The materials used in the AFRL setup, in order of increasing density, were extruded polystyrene (32 kg/m^3), vermiculite (126.4 kg/m^3), fiberboard (256 kg/m^3), water (998 kg/m^3), and sand.

Two modifications were made to the AFRL setup for use here. First, the AFRL research showed that copper projectiles did not penetrate past the fiberboard section. So, the sand was omitted from the S&T setup, however, a barrel of water was still included, in case the projectiles traveled farther than expected. The second modification of the AFRL setup was a substitution for the fiberboard. Fiberboard with the correct density could not be obtained locally, so after considering several materials with close to the desired density, cardboard bales were chosen as a substitute material. The cardboard bales used have an average density of 336 kg/m^3, and were readily available at reasonable cost.

The materials were lined up and leveled before the first shot, and realigned after each subsequent shot as necessary. The cardboard bales were shifted horizontally after each shot to minimize the chances of one projectile striking another. All five projectiles were successfully captured within the first cardboard bale without striking one another. After all shots had been completed, the bale was carefully disassembled in order to remove the projectiles.

All EFPs were fired from a standoff of 5.6 m (18.5 ft) and the speeds were recorded using a Phantom V5.1 high speed camera and reference board. Figure 3shows a conceptual sketch of the capture setup and a picture of the setup prior to the first shot.
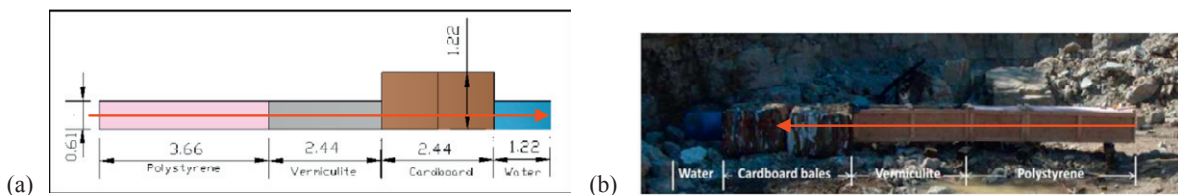

Fig.. 3. (a) Method 2 conceptual sketch, and (b) a photograph of the setup of method 2 prior to the first shot

3. Results

Table 1 shows the ten results obtained from the two recovery methods, five results from each recovery method. Method 1 was unable to determine the projectile's position when it stopped. Therefore, the penetration depth of the recovered projectile is only accurate to the length of a particular barrel, 0.9m. Method 2 was able to suspend the projectile in the

media, once the projectile stopped. Therefore, Method 2 was able to obtain the precise depth the projectile penetrated into the recovery method. The photographs of the recovered projectiles shown in Table 1 are on a 2.54 cm (1in) grid.

The recovered masses, cross-sectional areas and projectile length are similar for all ten projectiles. However, the five projectiles recovered from Method 1 do not have the same shape as the projectiles recovered with Method 2. The projectile from Method 1 shot 4 appeared to have rolled while penetrating the water of barrel one, so the tail of the projectile was removed during the penetration of the second polyethylene layer. The variations in the projectiles' shapes generated the need to investigate the forces acting on the projectiles during the deceleration process from each recovery method.

The differences in velocities are most likely an effect of the method used to measure the velocity, in which the analysis software requires the researcher to select a point on the projectile as the traverses through the recorded frames. The selection of points is subjective to the researcher, and as different researchers conducted the two methods, there stands to be a variation in the recorded velocities. Therefore, the force calculations use the average velocities, projectile weights recovered and cross-sectional areas. The force calculations for each method and a comparison of the forces acting on the projectiles are in the following section.

4. Analysis

4.1 Calculation procedure

The calculations of the forces acting on the projectiles use the conservation of energy approach as no times were recorded with either recovery method. The initial velocities for each recovery method analysis are the averages of the five velocities recorded with the high-speed camera. For calculation purposes, the authors assumed no projectile material was lost during the recovery process. Therefore, the initial projectile mass (M_0) equals the residual projectile mass (M_{rp}). For method 2, M_{rp} is the average mass of the five projectiles recovered and for method 1 M_{rp} is the average mass of shots 1, 2, 3, and 5.

The removal of shot 4's projectile mass, from the average mass of Method 1, is due to the substantial loss of the projectile's mass and including this projectile in the calculations resulted in substantially lower forces acting on the projectiles. In addition, the following calculations assume normal incidence to each segment of the recovery methods, therefore β in Equation 2, below, equals zero.

When these tests were conducted, there was no intent to compare the forces acting on the projectiles by each method. Since only the characteristics of the recovered projectile were needed, no velocities were measured as the projectile traveled through the materials in each method. The difference in analysis of the two recovery methods, is that Method 2 does not utilize impact dynamics. Section 4.2 summarizes the calculated forces acting on the projectile from each recovery method.
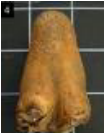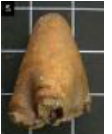
4.1.1   Calculation procedure for recovery Method 1

This analysis uses a conservation of momentum and energy approach. The analysis of the forces acting on a projectile recovery Method 1 requires both impact and fluid dynamics. Impact dynamic calculations identify the forces acting on the projectile as it penetrates the polyethylene segments of the recovery method, and fluid dynamic calculations identify the forces acting on the projectile as it passed through the water segments. The polyethylene segments had evidence of petalling when the projectile passed through the segment, indicating that the projectile penetrated the segment and impact dynamics were required to analyze the forces acting on the projectile as it penetra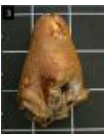ted the polyethylene segments. Figure 4 illustrates the petalling of the polyethylene segments. As the construction of the recovery method consists of alternating segments of polyethylene and water, the analysis will consist of alternating impact dynamics and fluid dynamics.

Fig. 4. Illustrates the petalling of the polyethylene segments.

Table 1. Results from both recovery methods[2]

Shot	Velocity (m/sec)	Recovered Mass (kg)	Recovered Mass (% initial)	Location Recovered	Cross-sectional area (cm^2)	Projectile Length (m)	Recovered Projectile Photographs
Method 1 Shot 1[2]	1234	0.34	78.7%	Second Barrel	24.39	0.073	
Method 1 Shot 2	1204	0.34	78.7%	Second Barrel	27.87	0.083	
Method 1 Shot 3	1175	0.31	72.2%	Second Barrel	22.80	0.07	
Method 1 Shot 4	1184	0.13	29.4%	Second Barrel	15.51	0.044	
Method 1 Shot 5	1210	0.34	78.7%	Second Barrel	25.18	0.076	
Method 2 Shot 1	1288	0.381	84.11%	0.67 meters into the cardboard	22.88	0.076	
Method 2 Shot 2	1310	0.374	83.48%	0.83 meters into the cardboard	20.27	0.064	
Method 2 Shot 3	1310	0.371	82.26%	1.21 meters into the cardboard	17.81	0.076	
Method 2 Shot 4	1302	0.371	82.26%	0.70 meters into the cardboard	13.38	0.076	
Method 2 Shot 5	1305	0.371	82.26%	0.90 meters into the cardboard	17.81	0.07	

Throughout this analysis, the exit velocity of a segment becomes the initial velocity of the successive segment. The calculations continue until the velocity becomes zero or the projectile loses the ability to penetrate the successive media. As shown by the results, each projectile stopped in the second barrel. Therefore, the calculations continued until the velocity of

[2] The pictures of the projectiles from Method 1 shots 1-3 are halved projectiles, when intact these projectiles have a similar appearance to the projectile of Method 1 shot 5.

the projectile was lower than the ballistic limit velocity (V_b) of the third polyethylene segment. Below are the calculations for both the polyethylene and water forces.

Impact Dynamics: The total kinetic energy (KE) of a projectile penetrating a target is the sum of the residual KE and the impulse transmitted to the target due to shear strength of target material [6]. The impulse transmitted is a function of the KE of any material lost, the elastoplastic deformation energy associated with the impact of the residual penetrator mass (M_r), the mass of the target (m) as if m were an unconstrained mass (E_f), and the elastoplastic deformation energy due to m being constrained by the plate (W_s) [6]. The authors used Equation 1 to calculate the total KE of a projectile penetrating a target [6].

$$M_0 V_0{}^2 = \frac{(M_r + m)V_{rp}^2}{2} + \frac{(M_0 + M_r)V_0^2}{2} + E_f + W_s \tag{1}$$

Where m is:

$$m = \rho_t A_f T sec(\beta) \tag{2}$$

The work imparted on the projectile penetrating the target (W_p) is the sum of E_f and W_s. Assuming that no material is lost and substituting W_p for E_f and W_s, Equation 1 can be used to obtain W_p by subtracting the residual kinetic energy (KE_{rp}) from the projectile's initial kinetic energy (KE_0).

$$W_p = M_0 V_0^2 - \frac{(M_r + m)V_{rp}^2}{2} \tag{3}$$

Equation 4 relates the residual velocity of the projectile after exiting the polyethylene segment (V_{rp}) to the initial velocity (V_0), ballistic limit velocity, the incidence angle (β), the residual penetrator mass, and the mass of the target [6].

$$V_{rp} = \frac{(V_0^2 - V_b^2)^{1/2} cos\beta}{1 + {m}/{M_r}} \tag{4}$$

The ballistic limit velocity is the velocity at which a projectile will penetrate a target fifty percent of the time [6]. Equation 5 calculates the ballistic limit velocity used in Equation 3 to calculate V_r [7].

$$V_b = \frac{\pi\Gamma\sqrt{\rho_t\sigma_e}D^2 T}{4M_r}\left[1 + \sqrt{1 + \frac{8M_r}{\pi\Gamma^2\rho_t D^2 T}}\right] \tag{5}$$

After obtaining W_p, Equation 6 calculates the force imparted on the projectile from the target.

$$F = \frac{W_p}{T} \tag{6}$$

This procedure is repeated twice, once for both the 2 mm thick initial polyethylene segment and the 4 mm thick second polyethylene segment. Once the velocity of the projectile is below V_b, the projectile is no longer considered capable of penetrating the third polyethylene segment and this segment imparts the final stopping force. The kinetic energy due to the residual projectile mass and velocity is the initial kinetic energy of the projectile as it enters the water segments of the recovery method.

Fluid Dynamics: Equation 7 calculates the force acting on the projectile as it travels through the water segment of recovery Method 1 [8]. Knowing that the projectile stopped in the second barrel, adjustments were made to the drag coefficient (C_{Dw}) of water so that the residual velocity of the projectile, at the end of the second water segment, was lower than the ballistic limit velocity of the third polyethylene segment. This empirically obtained drag coefficient is 0.18, which is substantially lower than the drag coefficient calculated based on the projectile's shape and Mach number. This low drag coefficient is from the hypervelocity projectile traveling through the water, generating an internal water pressure greater than the tensile strength of the polyethylene, resulting in the barrel rupturing and the water moving away from the projectile. The cross-sectional area of the projectile's tail (A_f) was measured from the collected projectile. The residual velocity from the penetration of the polyethylene segment is the initial velocity for this equation.

$$F = \frac{C_{Dw} A_f \rho_t V_{rp}^2}{2} \tag{7}$$

Equation 8 calculates the work imparted on the projectile as it travels through the water (W$_w$), assuming the force calculated in Equation 7 is a constant force acting on the projectile as it travels the length of the segment (L).

$$W_w = F * L \tag{8}$$

Equation 9 calculates the residual kinetic energy of the projectile penetrating the water segment, by subtracting the work imparted by the water from the residual kinetic energy of the projectile penetrating the previous polyethylene segment.

$$KE_{rw} = KE_{rp} - W_w \tag{9}$$

Equation 10 obtains the residual velocity of the projectile after it penetrated the water segment (V$_{rw}$). This velocity becomes the initial velocity for the successive impact dynamic calculations.

$$V_{rw} = \sqrt{\frac{2KE_{rw}}{M_r}} \tag{10}$$

This procedure is repeated for each water segment the projectile passed through. Recovery Method 2 utilizes equations similar to Equations 7-10, to calculate the forces acting on the projectile. The following sub-section details the utilization of these equations.

4.2 Calculation procedure for recovery Method 2

Method 2 also used a energy-momentum balance to calculate the approximate forces exerted on the projectile during deceleration through the soft recovery materials. Since both the initial velocity and mass of each projectile is known, the initial KE of each projectile can be calculated by the basic relationship in Equation 11.

$$KE_o = \frac{1}{2} V_0 M_0^2 \tag{11}$$

As with the analysis of recovery Method 1, Equation 11 uses the average velocity, projectile mass of the ten tests. No copper fragments other than the projectiles were discovered during dismantling of the soft recovery system.

Since the polystyrene, vermiculite, and cardboard bales were placed in contact with each other, it is assumed that all of the reduction in KE of the projectile occurs from the drag force acting on the projectile by the media. The drag coefficients used for the calculations are the drag coefficients acting on the copper projectile obtained by Lambert, et.al. [1], and are as follows: polystyrene: 0.77, vermiculite: 0.94, and fiberboard: 0.76. Since the cardboard bales had a higher density than did the fiberboard, several methods of estimating the drag coefficient were investigated. However, without measured velocities or material properties that area available for well characterized materials, a drag coefficient for the cardboard bales could not be calculated. The procedure for estimating the force exerted on the projectile in the cardboard section will be addressed shortly.

An iterative process using Equations 7-10 was used to calculate the force, work, residual KE, and residual velocity of the projectiles at several points along the penetration path. Since the drag coefficient for cardboard could not be empirically determined, nor calculated with the available material properties, and the fiberboard drag coefficient is not applicable, the forces on the projectile in the cardboard bale are only an estimation. Knowing the total distance that the projectile traveled in the cardboard, and estimating the velocity of the projectile when it enters the cardboard section, the average force on the projectile can then be calculated.

4.3 Calculated Forces

Given that the projectiles obtained from recovery Method 2 closely resemble the copper projectiles collected by Lambert et al, and the same EFP design was used in both recovery methods addressed in this paper, the variation in the shape of the projectiles in Method 1 from the shape of projectiles in Method 2 is assumed to have been a result of the different forces imparted on the projectile by recovery Method 1 versus Method 2. A compilation of the values obtained from the calculations previously discussed is in Tables 2 and 3.

Table 2 depicts the calculated forces acting on the projectiles in recovery method 1, in addition to the changes in kinetic energy and velocity. There is an order of magnitude difference between the forces acting on the projectile from the first

polyethylene segment and the first water segment. With this substantial force acting on the projectile for two microseconds, the reduction in velocity was only 1.5%. At the lower velocities, the polyethylene segments had a greater impact on the velocity reduction. However, the significant velocity reductions were from the water segments of this recovery method, as each segment reduced a projectile's initial velocity by 80%.
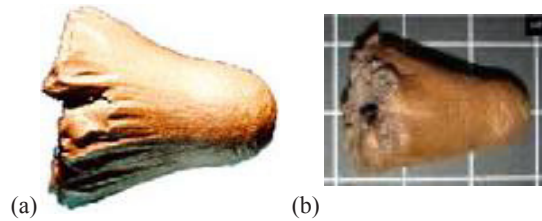

(a)   (b)

Fig. 5. Illustrates the similarity of the projectiles obtained from Lambert et al [1] (a) and recovery Method 2 (b).

Table 2. Force analysis of recovery Method 1.

Segment	Distance (m)	Initial Kinetic Energy (Kg*m²/sec²)	Work (Kg*m²/sec²)	Residual Kinetic Energy (Kg*m²/sec²)	Force (kg*m/sec²)	Residual Velocity (m/sec)
Initial Condition	0.000	261,073	0	261,073	0	1,252
2 mm Polyethylene	0.002	261,073	5,724	255,349	2,816,765	1,236
1st Water segment	0.881	255,349	250,836	4,513	285,500	165
4 mm Polyethylene	0.885	4,513	515	3,997	126,800	154
2nd Water segment	1.763	3,997	3,880	117	4,416	26
Final	1.763	117	117	0	Not Calculated[3]	0

Table 3. Force analysis of recovery Method 2.

Segment	Distance (m)	Initial Kinetic Energy (Kg*m²/sec²)	Work (Kg*m²/sec²)	Residual Kinetic Energy (Kg*m²/sec²)	Force (kg*m/sec²)	Residual Velocity (m/sec)
Initial Condition	0.000	261,073	0	261,073	0	1,252
Polystyrene	1.22	261,073	49,492	211,581	40,567	1,127
Polystyrene	2.44	211,581	40,110	171,471	32,877	1,015
Polystyrene	3.66	171,471	32,506	138,965	26,644	914
Vermiculite	4.88	138,965	126,630	12,334	103,795	272
Vermiculite	6.10	12,334	11,240	1,095	9,213	81

The forces acting on the projectile as it traverses recovery Method 2 are substantially lower than that of recovery Method 1.

Figure 6 depicts the change in kinetic energy over the distance of both recovery methods, in addition to a plot of the change in kinetic energy due to a constant force acting on the projectiles. Due to the length of recovery Method 1, there is a higher constant force associated with it than recovery Method 2. The slope between each segment is the force segment acting on the projectile. The changes in kinetic energy due to the forces of recovery Method 2 fit closely to the plot of the

---

[3] The stopping force acting on the projectile, from the third polyethylene segment was not calculated due to the absence of the distance the projectile penetrated and the time the force was acting on the projectile.

change in kinetic energy due to a constant force acting on the projectile, whereas Method 1 does not fit closely to the change in kinetic energy due to a constant force acting on the projectile.

The calculated constant force is the initial kinetic energy divided by the total distance the projectiles traveled, treating the recovery system as a whole. The change in energy for Method 2 follows the calculated constant force acting on the projectile, where the change in energy for Method 1 does not. The increased force acting on the projectiles from the polyethylene segments of Method 1, provide insight as to where the deformations are occurring.
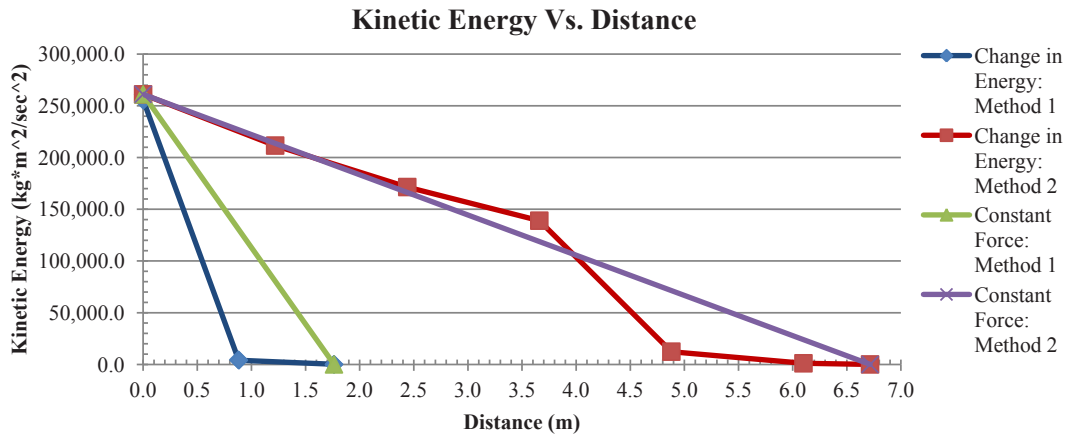

Fig. 6. A graphical representation of the change in kinetic energy due to the forces acting on the projectile as it travels through the two recovery methods.

5. Conclusion

The previously discussed calculations assume the projectiles impact each layer with normal impedance. However, the deformations of the projectiles recovered from Method 1 indicate that the projectiles did not impact every layer with normal impedance. The turbulence of the projectile traversing the water segment of recovery Method 1 caused the projectile to tumble. In some cases, the projectile turned in the second water segment, resulting in the projectile impacting the third polyethylene segment side-on, which would result in a flattening of one side depending on how it impacted the segment.

In the case of shot 4, from recovery Method 1, the projectile turned so that the tail of the projectile impacted the second segment prior to the tip of the projectile, which resulted in a substantial loss of the projectile's mass. In several cases, the projectile exited the side of barrel 2 resulting in the projectile impacting the stone wall behind the recovery method and the shot needing to be repeated. This provides evidence that the projectiles did not impact the second polyethylene segment at normal incidence, which would result in flattening effect of the projectile.

Figures 7 and 8 below demonstrate the differences between the projectiles recovered using Method 1 and Method 2. The projectiles recovered using method 1 are flatter and are not symmetric around the long axis as are the projectiles recovered using Method 2, despite the fact that all of the projectiles have very similar masses. If the change in kinetic energy of the projectile, shown in Fig. 6, is considered, it is clear that the projectiles in Method 1 experienced a much more rapid deceleration than did the projectiles in Method 2. While the force acting on each projectile over a unit distance is not explicitly illustrated, the change in kinetic energy is closely related to the force imparted on the projectile by the media it travels through. The flattening of the projectiles recovered using Method 1 is most likely due to the larger magnitude of force exerted on the projectile during the deceleration. In some cases, the tumbling or turning of the projectile within a barrel would result in a damaged projectile from an oblique impact on the rear polyethylene barrel surface.

Unlike Method 1, the kinetic force vs. distance profile of Method 2 shows a more constant reduction in kinetic energy, along the distance of travel. The lower magnitude of force exerted on the Method 2 projectiles appears to have not exceeded the shear strength of the copper, resulting in the un-deformed projectile that is fairly symmetric over its long axis, as shown in Fig. 8 (a) and (b). The absence of a very large reduction in velocity during the initial entry into the soft recovery system is undoubtedly the major factor in whether an un-deformed projectile is recovered.
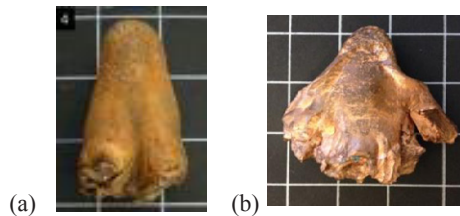
Fig. 7. Illustrates the flattening of the projectile from impacting the polyethylene not at normal incidence by comparing a projectile from Method 2 (a) with a flattened projectile from Method 1 (b).
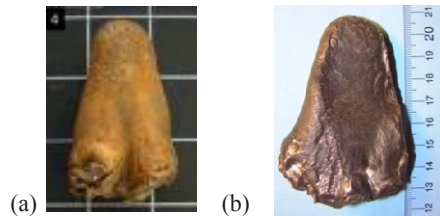

Fig. 8. Illustrates the damage imparted on theprojectile from impacting the third polyethylene segment by comparing a projectile from Method 2 (a) with a flattened projectile from Method 1 (b).

Each soft recovery method has pros and cons which must be considered by the researcher prior to choosing one method over the other. Method 1 uses widely available, low cost materials that can be setup quickly, and does not require a large space for setup. However, each barrel can only be used one time, after which, the entire setup must be redone with new barrels. The projectiles recovered using method 1 can be used to determine the final mass, but not the final geometry of projectiles produced by a certain EFP design. Method 2 is more costly than Method 1 and also requires more time to construct. Method 2 also requires almost an additional six meters of space for setup. A small test area may not be able to accommodate the entire length of material plus the standoff needed for the projectile to fully form. Even though the setup times for method 2 are significantly longer than method 1, if the researcher plans accordingly, multiple shots can be performed quickly using method 2. As shown in Fig. 8, the projectiles recovered using Method 2, do not appear to have undergone any noticeable deformation while traveling through the soft recovery media.

While there are some obvious differences in the projectiles recovered with the two methods, there is also one important similarity. Despite the final geometrical differences, the final masses of the projectiles are very similar. If cost, material availability, or a fast initial setup time is the most important consideration for the project, method 1 may be the best choice. If accurate projectile geometry or the ability to do several shots in a short period of time are the highest priorities, Method 2 would be the best choice.

References

[1] Lambert D., Mathew P., Jones S., Muse J., "Soft-Recovery of Explosively Formed Penetrators," 22nd International Symposium on Ballistics, Vancouver, BC, Canada, 2005

[2] Voort M., Rhijnsburger M., 2009 "IED Effects Research at TNO Defense Security and Safety," 13th International Symposium on the Interaction of the Effects of Munitions with Structures

[3] Mulligan P., "The Effects of Select Physical Parameters on an Explosively Formed Projectile's Performance", A thesis, Missouri University of Science and Technology, 2008

[4] Bookout L., "Impact Effects of Explosively Formed Projectiles on Normal and High Strength Concrete", A thesis, Missouri University of Science and Technology, 2011

[5] Blow molding: 55 gallon drums, industrial tanks: High Density Polyethylene Extra High Molecular Weight Hexane Copolymer, Thornton Prime Polymers, "online access" (http://thorntonandcompany.com/DataSheets/TPP95000.pdf), March, 30th 2012

[6] Zukas, Jonas A., 1990. High Velocity Impact Dynamics, John Wiley and Sons, INC. New York, USA

[7] Villanueva G., Cantwell W., 2003, The high velocity impact response of composite and FML-reinforced sandwich structures, Journal of Composites Science and Technology 64, p. 35

[8] Cooper, Paul W., 1996. Explosive Engineering, Wiley-VCH, Inc. New York, USA